Available online at www.sciencedirect.com
SCIENCE DIRECT
Polymer 47 (2006) 2526–2532
polymer
www.elsevier.com/locate/polymer

Solvent effects on the elasticity of polysaccharide molecules in disordered and ordered states by single-molecule force spectroscopy

Qingmin Zhang, Piotr E. Marszalek *

Department of Mechanical Engineering and Materials Science, Center for Biologically Inspired Materials and Material Systems, Duke University, Durham NC 27708, USA

Received 2 December 2005; received in revised form 7 December 2005; accepted 9 December 2005
Available online 3 February 2006

Abstract

Single-molecule force spectroscopy, especially as implemented on an atomic force microscopy (AFM) platform is unique in its ability to apply small ($F < 10$ pN) and large ($F > 1000$ pN) stretching forces to individual polymer chains and in this way examines their elasticity and also reports force-induced conformational transitions in whole polymers and in their building blocks. In this paper, we briefly review recent applications of single-molecule force spectroscopy to the study of polysaccharides elasticity. We provide examples illustrating AFM measurements of solvent effects on the hydrogen bonding and the elasticity of individual polysaccharides and how molecular dynamics simulation can aid the interpretation of AFM results. We also discuss the use of single-molecule force spectroscopy in exploring ordered secondary structures of individual polysaccharide chains and their multi-strand complexes.

Keywords: Polysaccharide; Single-molecule force spectroscopy; AFM (Atomic force microscopy)

1. Introduction

The development of laser trapping techniques in the 1970s and surface probe microscopy scanning tunneling microscopy (STM and AFM) atomic force microscopy, in the 1980s revolutionized polymer research in that it allowed not only visualization but also mechanical manipulations of individual polymer molecules. The uniqueness of atomic force microscopy, among these techniques is in its capability of applying very large stretching forces to individual polymers, and in this way measuring their elastic properties not only in the entropic regime characterized by the freely jointed chain (FJC)-like behavior but also in various enthalpic regimes characterized by large deviations from the FJC-type behavior, where force-induced conformational transitions of whole polymer chains and their components are triggered. These types of stretching measurements of polymers evolved into single-molecule force spectroscopy, which examines the relationship between a polymer length (end-to-end distance) and tension. Among biopolymers studied with the use of AFM-based single-molecule force spectroscopy, polysaccharides revealed a particular wealth of conformational behaviors that could be controlled by external forces [1–11]. For example, AFM stretching measurements captured forced chair-to-boat transitions of the pyranose ring in α-1,4 and α-1,6-linked glucose-based polysaccharides such as amylose, and dextran [2,4,7,12], chair-to-inverted chair transitions of α-D-galactose in such polysaccharides as pectin [8] and λ-carrageenan [10,11] and forced rotations around the C5–C6 bond of D-glucose in β-1,6-linked pustulan [3].

Because polysaccharides have an abundance of hydroxyl, acidic and charged groups they are prone to form regular/ordered structures such as single or multiple helices that are stabilized by hydrogen bonds, ionic bridges and also van der Waals interactions. AFM measurements proved invaluable in determining fingerprints of helical structures generated by polysaccharides such as carrageenans [13] Curdlan [14], and Xanthan [9] and even differentiated between their ordered and random coil structures. Consistent with previous measurements of the bulk properties of these polysaccharides, single molecule studies with the AFM also determined that their structures are profoundly affected by solvents and ionic conditions of the solution. The scope of this paper is to briefly review the recent progress in elucidating solvent effects on the hydrogen bonding and the elasticity of individual polysaccharide molecules and their complexes

* Corresponding author. Tel.: +1 919 660 5381; fax: +1 919 660 8963.
E-mail address: pemar@duke.edu (P.E. Marszalek).

0032-3861/$ - see front matter © 2006 Elsevier Ltd. All rights reserved.
doi:10.1016/j.polymer.2005.12.088

(multiple helices) obtained primarily by AFM-based single-molecule force spectroscopy and molecular dynamics simulations.

2. Materials and methods

2.1. Materials

Several polysaccharides were used in this study: amylose (type III, from potato, Sigma-Aldrich), pectin (from citrus, Sigma), pustulan (from lichen, Carbomer, San Diego, CA), dextran (Pharmacia/Pfizer, Peapack, NJ). Amylose triacetate was kindly provided by Prof. Yasuhiro Takahashi of Osaka University, Japan. Polysaccharides were first dissolved in proper solvent to form a solution at a concentration of 0.02–5%. To adsorb polysaccharide molecules onto a substrate, a drop of solution was placed on a clean glass substrate and dried. The sample was then rinsed intensely with water to remove most of the molecules and leave only these, which adsorbed tightly to the substrate [9]. The sample was placed in the AFM and proper solvent (such as water (dielectric constant, $\varepsilon = 80$), dimethyl sulfoxide (DMSO) ($\varepsilon = 47.2$), hexadecane ($\varepsilon = 2.0$), or dimethyl carbonate (DMC, $\varepsilon = 3.1$)) was injected into the liquid chamber.

2.2. Single molecule force spectroscopy

Force spectroscopy measurements were carried out on a home-made AFM instrument. This AFM was equipped with an AFM detector head from the MultiMode AFM (Veeco, USA) and a single-axis piezoelectric actuator with an integrated strain gauge sensor from Physik Instrumente (Germany). The spring constant of each Si_3N_4 cantilever (Veeco) was calibrated using the energy equipartition theorem [15]. To pick up a single polysaccharide molecule for stretching measurements, the AFM tip was pressed against the substrate at a force of 1–40 nN for several seconds and subsequently withdrawn.

2.3. Steered molecular dynamic simulations

SMD simulations [1,3,4,6] of amylose, pustlan and dextran and data analysis were carried out with the programs NAMD2 [16], XPLOR [17], VMD [18] and a new CHARMM-based carbohydrate solution force field [19]. Briefly, AFM stretching measurements on individual polymers are modeled in the SMD protocol by fixing one terminal of the polymer and applying an external harmonic potential to the other terminal. The center of this harmonic potential moves at a constant velocity in the stretch direction simulating the movement of the AFM cantilever. For details on these simulations refer to [4].

2.3.1. Normalization of force–extension curves

Because the contour lengths of each polysaccharide fragment, which is picked up randomly by the AFM tip, is different, force–extension curves obtained by the AFM need to be normalized to compare the results. Briefly, this extension normalization procedure is based on the property of the FJC-model that predicts chain extension at any force to be proportional to its contour length. Thus, by assuming that the extension of a polysaccharide chain, at a given force that is common to all the recordings, is equal to one, we can eliminate the dependence of the shape of the force curve on the particular value of the contour length. Details are available in our previous papers [1,6]. In addition, for these polysaccharides for which we carried out SMD simulations we can use the SMD results to normalize the chain extension with respect to a single sugar ring. This is done by measuring, from the simulation, an average projection of the distance between the consecutive glycosidic oxygen atoms on the direction of the force at the highest stretching forces ($\sim$3000 pN), at which conformational transitions (if any) of the sugar rings have already completed [1]. For example, the average distance between the oxygen atom # 4 on the first ring and the oxygen atom #1 on the 10th ring of an amylose fragment, projected on the direction of a SMD force of 3270 pN was determined to be 55.7 Å, and this length was found to be independent on the dielectric constant of the solvent used in the simulation. This result gives an average extension of amylose at $F = 3270$ pN to be 5.57 Å per ring, which then can be used to normalize the experimental force curves (assuming that the stretching force of 3270 pN or greater was achieved experimentally). This normalization is very convenient because it reports the elastic properties of polysaccharide chains 'per ring' and can be used to compare the results obtained on different fragments, under different (solvent) conditions. Details can be found in the supporting material to Ref. [1].

2.4. Other methods

For more information on the materials and methods used by other authors whose results are discussed in this review, the reader is referred to the original papers.

3. Results and discussion

3.1. Amylose elasticity in high and low dielectric constant solvents

Amylose is a linear 1→4-linked α-D-glucan (Fig. 1(a), inset). The force–extension curves of amylose obtained by AFM in water (dielectric constant, $\varepsilon = 80$) display a characteristic plateau feature at about 280 pN (see Fig. 1(a), black curve) [2]. Thus, the elasticity of individual amylose chains deviates strongly from the entropic elasticity expected of simple FJC-type polymers. This plateau feature was attributed to the force-induced chair-to-boat transitions of the glucopyranose rings, which lengthen the contour length of amylose by about 17% [2].

The close proximity of hydroxyl groups from neighboring rings in amylose implies that they should be able to form hydrogen bonds (H-bonds). In water these bonds will not be very strong because of the competition of glucose hydroxyls to form hydrogen bonds with water molecules. However, we expected that solvents with a very low dielectric constant should stabilize these inter-residue H-bonds. To investigate if

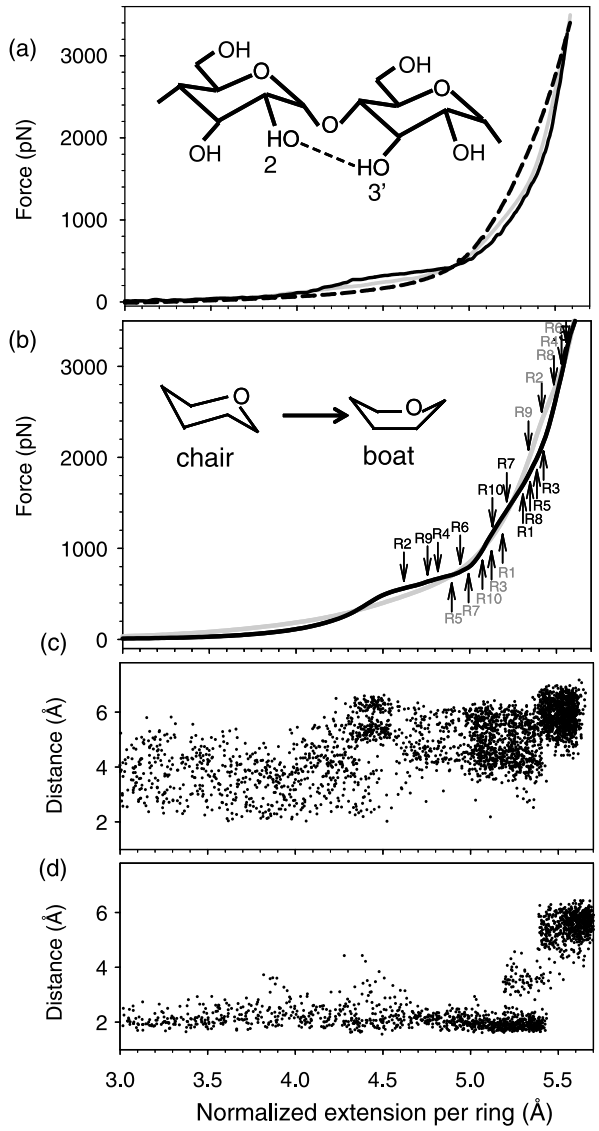

Fig. 1. (a) Experimental force–extension curves of amylose in water (black trace), in DMSO (gray trace) and in DMC (dashed trace). The inset shows the structure of amylose and the dashed line indicates the inter residue hydrogen bond. (b) SMD-obtained force–extension curves of an amylose fragment composed of 10 rings stretched in water (black trace) and in vacuum (gray trace). The arrows indicate the positions at which the individual rings undertake chair-to-boat transitions. The inset shows the schematic illustration of force-induced chair-to-boat transitions of the glucopyranose ring. (c) A typical SMD trajectory of the O2–H3′ distance between ring 2 and ring 3 of amylose in water ($\varepsilon=80$). (d) Same as (c) but in vacuum ($\varepsilon=1$). Adapted from [1].

such a stable H-bonding will affect the mechanical properties of amylose, we measured its force–extension curves in dimethyl sulfoxide (DMSO) ($\varepsilon=47.2$), dimethyl carbonate (DMC) ($\varepsilon=3.1$) [1] and in hexadecane ($\varepsilon=2.0$). Fig. 1(a) shows a comparison of typical force–extension curves of amylose in water (black trace), in DMSO (gray trace) and in DMC (dashed trace). The force–extension relationship obtained in hexadecane (not shown in Fig. 1) was similar to that obtained in DMC. The characteristic plateau at a force of 280 pN and extensions between 4.4 and 5.0 Å/ring, so pronounced in water, is reduced in DMSO and almost disappears in DMC, for which the force-curve runs below that in water; while at higher extensions (>5.0 Å/ring), the curve in DMC runs above the curve obtained in water. These results indicate that the elasticity of individual amylose molecules is solvent dependent. Although it is clear from Fig. 1(a), that DMC strongly affects the elasticity of amylose the mechanism of this change cannot be deduced just from AFM measurements alone.

3.2. SMD simulations of amylose elasticity in high and low dielectric constant solvents

To clarify the mechanism of solvent effects on amylose elasticity and to reveal conformational details of the behavior of the glucopyranose rings during the forced stretching process, we carried out steered molecular dynamic (SMD) simulations on an amylose fragment composed of 10 rings [1,12]. We carried out our simulations using the simplest implicit models for the solvents, namely by scaling the electrostatic and vdW interactions with a fixed dielectric constant, which assumed a value of 80 for water and one to represent other non-polar solvents (vacuum conditions). The results of two such simulations are shown in Fig. 1(b), where the force–extension simulation curves in water ($\varepsilon=80$) are depicted by the black solid line and the force curve obtained in a vacuum ($\varepsilon=1$) is depicted by the gray solid line. In both simulations, the starting conformation of the pyranose rings is the $^4C_1$ chair [20], while the final conformation of the stretched pyranose rings is a skew boat [1,12]. Clearly, the curve of amylose in water ($\varepsilon=80$) show an obvious plateau at the extension region of 4.4–5.0 Å/ring; while in a vacuum ($\varepsilon=1$), this plateau is not present. However, at higher extensions (>5.2 Å/ring), the curve obtained in a vacuum runs above the curve in the water. Thus, these simulation results are consistent with our AFM measurements. In Fig. 1(b), we marked the positions where the chair-boat transition occurred for each individual ring. Evidently, the transitions in the vacuum occurred much later, at higher extensions, than the transitions in water.

In the simulation process, we also monitored the length of the putative hydrogen bonds O2–H3′ (indicated in Fig. 1(a)) both in water and in vacuum [1] and we plot their history in Fig. 1(c) and (d). In water, the O2–H3′ distance oscillates between 2 and 5 Å before the chair-to-boat transition occurs and between 3.5 and 6.5 Å after the transition, indicating no persistent hydrogen bond between these atoms throughout the simulation (Fig. 1(c)) [1]. On the other hand, in vacuum, this distance stays within a small range of 1.7–2.4 Å before the conformational transition occurs. This result is indicative of a strong hydrogen bond between O2 and H3′ (Fig. 1(d)) [1]. During the conformational transition, this distance increases abruptly to about 5 Å (Fig. 1(d)) [1] indicating that the transition involves breaking of a bond between two rings. From these simulation results, it can be concluded that in solvents of high dielectric constant, the inter residue hydrogen bonds O2–H3′ are very weak as compared to solvents with very low dielectric constants. As a result, the strong inter residue hydrogen bonds between O2–H3′ atoms on adjacent amylose

rings rigidify the amylose backbone, clamp the rings together, and inhibit their transition to a boat-like conformation. In consequence these bonds modulate amylose elasticity by shifting the chair-to-boat transitions to higher forces/extensions as compared to the transitions, which occur in water in the absence of such strong inter-residue H-bonds.

3.3. ATA elasticity is solvent-independent

To verify our hypothesis regarding the role of the inter-residue hydrogen bonds in amylose elasticity, we performed similar measurements on amylose triacetate (ATA) that has three acetyl groups replacing three hydroxyl groups (Fig. 2, inset) [21]. This replacement abolishes the ability of neighboring sugar rings of ATA to form hydrogen bonds. Fig. 2 shows ATA force–extension curves obtained in water (black traces) and in hexadecane (gray traces). As we expected, the curves obtained in water and hexadecane now overlap very well. Similar results were obtained for ATA in DMC [1]. These results suggest that the elasticity of ATA is solvent-independent. Moreover, all of ATA force–extension curves obtained both in water in hexadecane and in DMC display now a prominent transition feature at ~280 pN making them very similar to the curves obtained on native amylose in water. This result provides strong support for our hypothesis that solvents affect amylose elasticity by modulating the strength of inter-residue hydrogen bonds [1].

3.4. How strong are H-bonds in amylose?

By comparing the experimental force–extension curves obtained in water and in DMC it is possible in principle to estimate the relative strength of these bonds. This can be achieved by calculating and comparing the work that the external force performs to extend the amylose chain to the same length per ring in both solvents. This work is equal to the area under the force–extension curve (Fig. 1(a)). Our SMD simulations show that the normalized extensions of amylose in water and in DMC become truly equal only at very high forces, $F > 3000$ pN (Fig. 1(b)). Thus, in order to correctly compare the work done in these two solvents it is necessary to achieve such high stretching forces experimentally. From the results shown in Fig. 1(a) and similar data, we found that on average the external force needs to carry out ~1.5 kcal/mol more work per ring to fully extend the amylose chain in DMC as compared to water [1]. This number is a very reasonable estimate for the energy of a single hydrogen bond in maltose (the building dimer of amylose) in DMC as compared to water. We would like to stress that this estimate is valid only for measurements such as shown in Fig. 1(a), where the stretching forces indeed exceeded 3000 pN. If, for example, the stretching forces had reached only ~ 2000 pN, and one would erroneously have assumed that amylose extensions in DMC and in water had been already equal at 2000 pN, as a result the DMC curve would have shifted right, and the area enclosed between the two curves, at the extensions between 5.0 and 5.5 Å/ring would have greatly decreased. Then, one could erroneously conclude that less work was done to stretch amylose in DMC than in water, contradicting the hypothesis about enhancing the strength of the internal H-bonds in amylose in DMC.

3.5. Pectin elasticity is solvent dependent

Pectin is a polymer composed of 1→4-linked α-D-galactopyranuronic acid (Fig. 3, inset). The galactopyranuronic acid ring has the same basic ring structure as α-D-glucose. However, while the C4–O4 bond is equatorial in glucose it is oriented axially in galactose. Another difference between amylose and pectin is that in pectin at C5 position an acid group is attached instead of an alcohol. This acid group and other hydroxyl groups have a strong tendency to form inter residue hydrogen bonds. The possible hydrogen bonds are shown in the inset of Fig. 3. To test whether these bonds could be strengthen in a low dielectric constant solvent we performed force spectroscopy measurements on pectin in DMSO and in

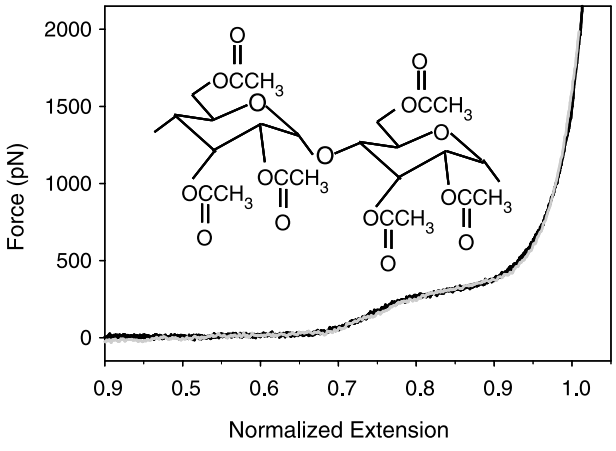

Fig. 2. Froce extension curves of amylose triacateate (ATA) in water (black trace) and in hexadecane (gray trace). The inset shows the structure of ATA.

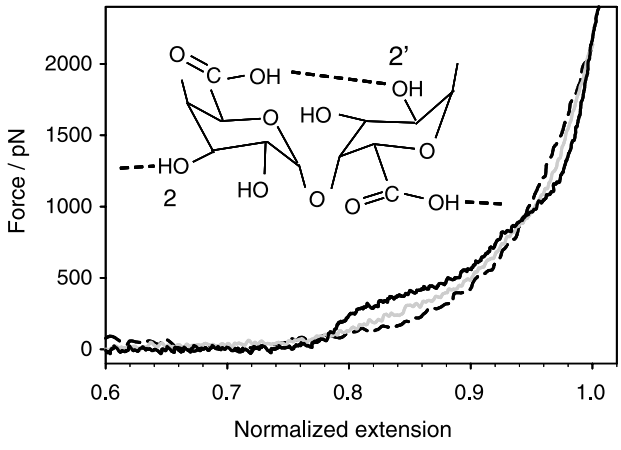

Fig. 3. Force extension curves of pectin in water (black trace), in DMSO (gray trace) and in hexadecane (dashed trace). (Inset) The structure of the building block of pectin.

hexadecane, and in Fig. 3 compared the obtained force curve (DMSO, gray trace; hexadecane, dashed trace) to that measured earlier on pectin in water (black trace) [8]. The force–extension curves of pectin obtained in water display two distinct plateaus at about 300 and 800 pN, which were attributed to the force-induced lengthening of the galactose ring by the chair inversion transition [23], which is composed of two reactions: chair-to-boat followed by a boat-to-an inverted chair conformational transition [8]. The force–extension curves obtained in DMSO and in hexadecane do not reveal any clear plateau pattern but these traces deviate from the curve in water indicating that the elasticity of pectin is indeed solvent dependent. The force curve obtained for pectin in hexadecane ($\varepsilon = 2.0$) runs below the curve measured in water ($\varepsilon = 80$) at intermediate extensions (4.5–5.3 Å/ring), and above the water force curve at higher extensions (>5.3 Å/ring) suggesting a solvent-controlled mechanism, similar to that experienced by amylose. Thus, it is tempting to speculate that the solvent dependence of pectin elasticity is related to the solvent-controlled modulation of the strength of inter residue hydrogen bonds. In low dielectric constant solvents (e.g. hexadecane), these hydrogen bonds are strong and, similar to amylose, are expected to shift the conformational transitions in the neighboring rings to higher forces/extensions as compared to water. Although the solvent effect on pectin elasticity is clearly similar to the effect observed for amylose, we did not attempt to estimate the strength of H-bonds in pectin in hexadecane. This is because the maximum experimental stretching force for pectin in hexadecane that we reached so far was only ~ 2000 pN, much less than 3000 pN at which we expect the normalized length to be solvent independent. Thus, it is likely that the length of pectin in hexadecane at ~2000 pN is actually less than in water at the same force and comparing the areas under the force curves would not produce a reliable estimation of the work per ring. To further verify these ideas SMD calculations and new experiments, including control experiments on substituted pectin are warranted.

3.6. The elasticity of 1→6-linked polysaccharides is solvent-independent

So far we discussed the results of force spectroscopy measurements and the effects of various solvents on the elasticity of polysaccharides in which the neighboring rings are linked by two bonds. Such linkages limit the distance between various acceptors and donors of putative H-bonds and facilitate their formation. However, some pyranose-based polysaccharides exploit 1→6-linkages that increase the separation of the rings by an extra bond (C5–C6). To test whether solvents with a low dielectric constant affect the elasticity of 1→6-linked polysaccharides, we performed a series of measurements on dextran and pustulan, which are α-1→6-linked and β-1→6-linked D-glucans, respectively (Fig. 4(a), inset, Fig. 4(b), inset).

The typical elasticity profile of dextran in water ($\varepsilon = 80$) is shown in Fig. 4(a) as the black trace, and somewhat like amylose, it has a pronounced plateau, except that it occurs at a higher force at about 800 pN [2,4,5]. Our work suggests that

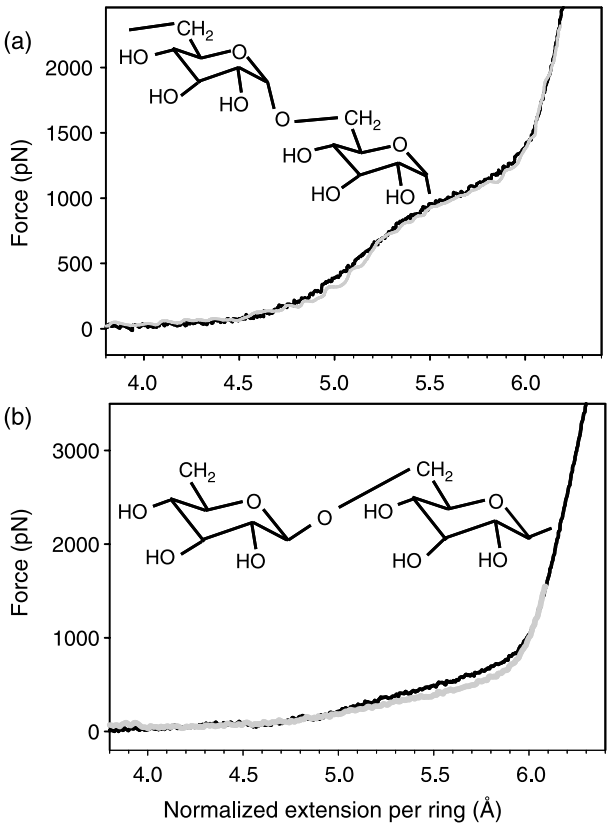

Fig. 4. (a) Force extension curves of dextran in water (black trace) and in hexadecane (gray trace). (Inset) The structure of dextran. (b) Force extension curves of pustulan in water (black trace) and in DMC (gray trace). (Inset) The structure of pustulan. Panel (b) adapted from Ref. [4].

this plateau reflects a force-induced lengthening of the O1–O6 distance through a compound conformational transition that involves the rotation about the C5–C6 bond and chair-to-boat-like transition of the glucopyranose ring [4]. The force–extension curve of dextran obtained in hexadecane ($\varepsilon = 2.0$) is shown as a gray trace in Fig. 4(a). It is clear that the force curve obtained in hexadecane is indistinguishable from the curve obtained in water. Thus, we conclude that hexadecane does not affect dextran elasticity.

The force–extension curve of pustulan in water is shown as a black trace in Fig. 4(b). Although, the curve does not reveal any plateau, which would be similar to those of amylose or dextran, it does not follow the FJC model of entropic elasticity either. Interestingly, at extensions between 4.7 and 5.9 Å/ring pustulan elasticity is almost hookean, with tension directly proportional to extension [3,4]. Our study proved that this linear elasticity is solely caused by the forced rotation about the C5–C6 bonds [3,4]. The force curve of pustulan in a low dielectric constant solvent, dimethyl carbonate ($\varepsilon = 3.1$), is also shown in Fig. 4(b) as a gray trace. It is evident that like dextran, pustulan elasticity is also solvent independent. These results support our initial conjecture that low dielectric constant solvents affect polysaccharides' elasticity by modulating the strength of inter-residue hydrogen bonds. If the formation of such bonds is prevented geometrically by separating acceptors

and donors, as seems to be the case for 1→6 linked polysaccharides, then the solvent effects are nullified.

3.7. Regular structures of polysaccharides studied with single-molecule force spectroscopy

3.7.1. The elasticity of random coils and helices of Xanthan

Xanthan is a bacterial polysaccharide whose primary structure consists of β-D-glucose rings substituted with trisaccharide side chains: O-β-D-mannopyranosyl-(1,4)-O-β-D-glucopyranosyl-uronic acid-(1,2)-6-*O*-acetyl-*a*-D-mannopyranosyl at C-3 position of every other glucose ring of the main chain [9]. Native xanthan forms ordered multiple helical structures with the number of strands in the helix presently unknown. Xanthan melts into a disordered single-strand coil at high temperatures (>90 °C) and this disordered state may be maintained by quenching hot xanthan solution on ice (denatured Xanthan) [9]. Li et al. used AFM-based single-molecule force spectroscopy to study the elasticity of individual Xanthan molecules in their ordered and disordered states [9]. They found that the elasticity of denatured Xanthan closely follows the FJC model. Interestingly, the elasticity of native Xanthan displayed a large deviation from the FJC model evident as a long plateau in the force–extension curve at a force of 400 pN (Fig. 5). This plateau was attributed to separating the strands within the multi-helical secondary structure of Xanthan or to forcing the helix to a significantly elongated state, similar to the B–S transition in the double helix of DNA [24]. This study for the first time demonstrated that single-molecule force spectroscopy could be very useful not only in investigating the mechanical properties of single polysaccharide chains but also their complexes forming regular secondary structures [9]. Since the native structure of Xanthan is stabilized by H-bonds and electrostatic interactions [9], it would be very interesting to test whether the elasticity of native Xanthan is affected by solvents with a low dielectric constant that are expected to further enhance these interactions.

3.7.2. The elasticity of random coils and helices of carrageenan

Carrageenans are linear polysaccharides composed of alternating α-1→4 and β-1→3-linked galactose residues [20]. It is well known that in water solutions carrageenan exists as a random coil. However, carrageenans undergo conformational transitions to more ordered, likely helical, structures after supplementing their solutions with various concentrations of salts, e.g. with 0.1 M NaI. Xu et al. studied the elastic properties of individual molecules of type-I carrageenan in pure water and in aqueous solutions containing 0.1 M NaI [13]. In water, carrageenan behavior was typical of a freely jointed chain with some segment elasticity [13]. However, in 0.1 M NaI the force–extension curves of carrageenan displayed a long plateau feature at 300 pN [13] similar to that observed for native Xanthan by Li et al. [9]. This plateau feature, which signaled a completely irreversible conformational transition of carrageenan was attributed to a forced unfolding of the carrageenan helix [13].

3.7.3. The elasticity of random coils and multiple helices of curdlan

Curdlan is a linear polysaccharide composed of β-1→3-linked D-glucose that crystallizes as a triple helix [14]. It dissolves well in alkaline solutions. At low concentrations of NaOH (<0.19 M) it exists as a triple helix and at high concentrations (>0.24 M) it denatures and exists as random coils. At intermediate concentrations curdlan structure is likely to be a duplex with a third strand somewhat separated [14]. Recently, Zhang et al. used AFM-based single-molecule force spectroscopy to investigate the elastic properties of curdlan in its various states by stretching curdlan molecules in solutions with varying concentrations of NaOH [14]. At high NaOH concentrations they found that curdlan behaves as a simple entropic spring, which is consistent with its predicted structure to be that of a random coil [14]. However, at low NaOH concentrations they found that the force–extension curves of curdlan displayed a striking plateau at 60 pN (Fig. 6). These very interesting results likely captured force-induced conformational transitions within the triple helix of curdlan that very much resemble the B–S transition plateau in DNA duplexes [24]. The study also reported that the plateau force decreased to 40 pN when curdlan was stretched at intermediate NaOH concentrations, and increased to 90 pN after the thermal treatment of curdlan, which is believed to enhance the hydrophobic interactions within the triple helix [14]. These studies further indicate the usefulness of single-molecule force spectroscopy in structural and conformational studies of polysaccharides.

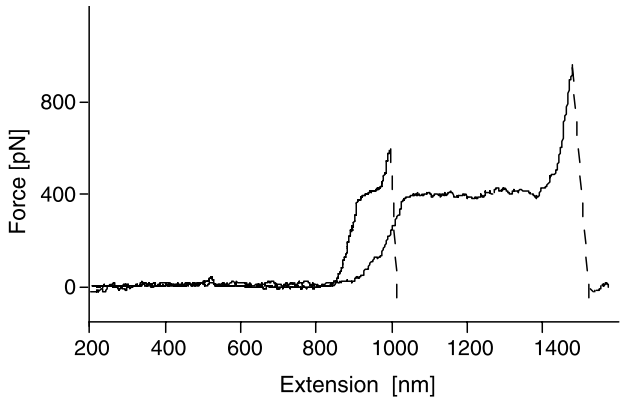

Fig. 5. Typical force–extension curves of native Xanthan [9] (with permission).

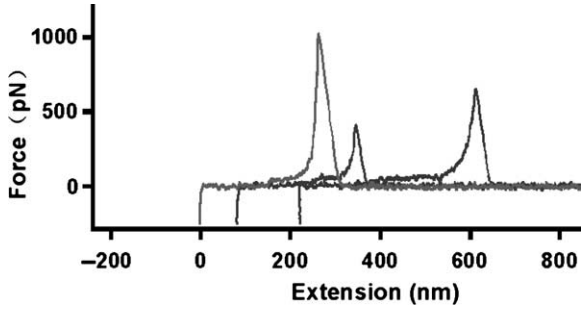

Fig. 6. Typical force–extension curves of curdlan in 0.10 M NaOH (aq) [14] (with permission).

3.7.4. Single-molecule force spectroscopy captures the formation of V-amylose helix in butanol and aqueous iodine solution

Amylose forms regular single stranded V-amylose helices in precipitates and crystals obtained from butanol and aqueous iodine solutions [25–30]. However, its structure in these solutions remains elusive mainly because amylose does not form molecular solutions in these solvents [31]. We used AFM-based single molecule force spectroscopy to stretch single amylose molecules in these poor solvents and probed amylose secondary structure in solution by examining its elasticity. We found that in butanol amylose forms compact helices whose elasticity is controlled by a network of intra-molecular hydrogen bonds. We determined that the pitch of the amylose helix in solution is 1.3 Å/ring, which is consistent with the result of X-ray measurements on amylose crystals. We also found that the force driving the formation of the helix in butanol is 50 pN [22]. In aqueous iodine solution amylose was found to form compact but mechanically weak helices whose elasticity displayed a significant hysteresis. Our AFM results were corroborated by SMD simulations of amylose elasticity in the explicit butanol solvent. Thus, AFM-based single molecule force spectroscopy, because of its unique capability of forcing polymers into solvents in which they normally do not dissolve, allowed us to capture regular conformations of amylose in butanol and iodine aqueous solution, which has been very difficult to obtain using traditional spectroscopic techniques [22].

4. Conclusions

In this paper, we have reviewed recent single-molecule force spectroscopy studies focused on solvent effects on the elasticity of several polysaccharides. Our experimental results reinforced by SMD simulations suggest that inter residue hydrogen bonds between adjacent sugar rings play crucial roles in solvent effects on the elasticity. Polysaccharides, which can form inter residue hydrogen bond, such as amylose and pectin, all display solvent dependent elasticity but the elasticity of their derivatives such as ATA, in which the formation of inter-residue H-bonds is inhibited chemically is solvent independent. Similarly, when H-bonds cannot form because of geometrical constraints, which exist in 1→6-linked polysaccharides such as dextran and pustlan, the elasticity of these polysaccharides does not depend on the dielectric constant of the solvent. Inter residue hydrogen bonds are weak in solvents with a high dielectric constant (e.g. water), but are strong in solvents with a low dielectric constant (e.g. hexadecane and DMC). The strengthened hydrogen bonds rigidify the polysaccharide backbone, decrease the flexibility of the neighboring rings around the glycosidic linkages and shift the conformational transitions of the sugar rings to higher forces. In addition our work and that of others suggest that single-molecule force spectroscopy is ideally suited to study the structural and mechanical properties of many polysaccharides in their ordered (helical) states, which are frequently induced by various solvents and solutes.

Acknowledgements

This work was supported by a grant from the National Science Foundation and by Duke University funds to PEM. We are grateful to Prof. Yasuhiro Takahashi of Osaka University, Japan for a sample of amylose triacetate.

References

[1] Zhang Q, Jaroniec J, Lee G, Marszalek PE. Angew Chem Int Ed 2005;44:2723–7.
[2] Marszalek PE, Oberhauser AF, Pang YP, Fernandez JM. Nature 1998;396:661–4.
[3] Lee G, Nowak W, Jaroniec J, Zhang Q, Marszalek PE. J Am Chem Soc 2004;126:6218–9.
[4] Lee G, Nowak W, Jaroniec J, Zhang Q, Marszalek PE. Biophys J 2004;87:1456–65.
[5] Rief M, Oesterhelt F, Heymann B, Gaub HE. Science 1997;275:1295–7.
[6] Zhang Q, Lee G, Marszalek PE. J Phys: Condens Matter 2005;17:S1427–42.
[7] Li H, Rief M, Oesterhelt F, Gaub HE, Zhang X, Shen J. Chem Phys Lett 1999;305:197–201.
[8] Marszalek PE, Pang YP, Li H, Yazal JE, Oberhauser AF, Fernandez JM. Proc Natl Acad Sci USA 1999;96:7894–8.
[9] Li H, Rief M, Oesterhelt F, Gaub HE. Adv Mater 1998;10:316–9.
[10] Marszalek PE, Li H, Fernandez JM. Nat Biotech 2001;19:258–62.
[11] Xu QB, Zhang WK, Zhang X. Macromolecules 2002;35:871–6.
[12] Lu Z, Nowak W, Lee G, Marszalek PE, Yang W. J Am Chem Soc 2004;(126):9033–41.
[13] Xu QB, Zou S, Zhang WK, Zhang X. Macromol Rapid Commun 2001;22:1163–7.
[14] Zhang L, Wang C, Cui S, Wang Z, Zhang X. Nano Lett 2003;3:1119–24.
[15] Florin EL, Rief M, Lehmann H, Ludwig M, Dornmair C, Moy VT, et al. Biosens Biolelectr 1995;10:895–901.
[16] Kalé L, Skeel R, Bhandarkar M, Brunner R, Gursoy A, Krawetz N, et al. Comput Phys 1999;151:283–312.
[17] Brunger A. X-PLOR, Version 3.1: A System for X-ray Crystallography and NMR. Yale University, New Haven, CT;1992.
[18] Humphery W, Dalke A, Schulten K. J Mol Graph 1996;14:33–8.
[19] Kuttel M, Brady JW, Naidoo KJ. Comput Chem 2002;(23):1236–43.
[20] Rao VSR, Qasba PK, Balaji PV, Chandrasekaran R. Conformation of Carbohydrates. Amsterdam: Harwood Academic Publishers; 1998.
[21] Takahashi Y, Nishikawa S. Macromol 2003;(36):8656–61.
[22] Zhang Q, Lu Z, Yang W, Marszalek PE. 2005; Submitted.
[23] Pickett HM, Strauss HL. J Am Chem Soc 1970;92:7281–90.
[24] Smith SB, Cui YJ, Bustamante C. Science 1996;271:795–9.
[25] Helbert W, Chanzy H. Int J Bio Macromol 1994;16:207–13.
[26] Bail PL, Rondeau C, Buleon A. Int J Bio Macromol 2005;35:1–7.
[27] Rappenecker G, Zugenmaier P. Carbonhydr Res 1981;89:11–19.
[28] Rundle RE, Edwards FC. J Am Chem Soc 1943;65:2200–3.
[29] Gessler K, Uson I, Takahai T, Krauss N, Smith SM, Okada S, et al. Proc Natl Acad Sci USA 1999;(96):4246–51.
[30] Rundle RE, Baldwin RR. J Am Chem Soc 1943;65:554–8.
[31] Hirai T, Hirai M, Hayashi S, Ueki T. Macromol 1992;25:6699–702.